Stochastic Environmental Research and Risk Assessment
https://doi.org/10.1007/s00477-018-1587-0

ORIGINAL PAPER

Trends and variability in African long-term precipitation

Charles Onyutha[1]

Abstract
African precipitation trends are commonly analyzed using short-term data observed over small areas. This study analyzed changes in long-term (1901–2015) annual and seasonal precipitation of high spatial (0.5° × 0.5° grid) resolution covering the entire African continent. To assess an acceleration/deceleration of the precipitation increase/decrease, trend magnitude (mm/year) over the period 1991–2015 was subtracted from that of 1965–1990 to obtain Slope Difference (SD, mm/year). Co-variation of precipitation sub-trends with changes in large-scale ocean–atmosphere conditions was investigated. Regardless of the trend significance, in most parts of Africa, annual precipitation exhibited negative (positive) trends over the period 1965–1990 (1991–2015). Thus, the continent was, on average, recently (from 1991 to 2015) wetter than it was over the period 1965–1990. From 1901 to 2015, the null hypothesis H_0 (no trend) was rejected ($p < 0.05$) for annual precipitation decrease over West Africa especially along the coastal areas near the Gulf of Guinea. The H_0 was also rejected ($p < 0.05$) for the increase in annual and September–November precipitation of some areas along the Equatorial region (such as in Gabon and around Lake Victoria). For both annual and seasonal precipitation, the least SD values in the range − 1 to 1 mm/year were obtained in areas north of 10° N. The SD value went up to about 20 mm/year over the Sahel belt especially for the peak monsoon (June–August season). For the March–May precipitation, positive SD values were obtained in the Western part of Southern Africa. However, negative SD values (around − 5 mm/year) were obtained in the Horn of Africa. Variation in sub-trends of the East African precipitation was found to be driven by changes in Sea Surface Temperature (SST) of the Indian and Atlantic Oceans. Variability in sub-trends of the West African precipitation is linked to changes in SST of the Atlantic Ocean. Changes in sub-trends of the South African precipitation correspond to anomalies in SST from the Pacific and Indian Oceans. Knowledge of precipitation changes and possible drivers is vital for predictive adaptation regarding the impacts of climate variability on hydro- or agro-meteorology.

Keywords Africa · Precipitation · Trend analyses · Sub-trends · Climate variability · Climate indices

1 Introduction

Analyses of precipitation changes are vital to obtain an insight on the influence of land–atmosphere interactions or climate system on hydro- or agro-meteorology (Onyutha and Willems 2015). In Africa (especially the sub-Saharan region), majority of people depend on smallholder farming for subsistence (International Water Management Institute [IWMI] 2014). However, agricultural practices in the sub-Saharan Africa mainly depend on rain-fed cropping system. Because rainfall plays a critical role in sustaining livelihoods and economic development across Africa, changes in rainfall intensity and the time of occurrence, or alteration in precipitation patterns can engender huge consequences on agriculture, and other societal or socio-economic aspects of various regions (Ogwang et al. 2015; Maidment et al. 2015).

For studies on changes in precipitation and related variables such as temperature or evapotranspiration in Africa, analyses were mainly confined to regional scale (see, for instance, Onyutha 2016a; Tierney et al. 2015; Diem et al. 2014; Jury 2013; Camberlin 2009; Lebel and Ali 2009; Korecha and Barnston 2007; Fauchereau et al.

Electronic supplementary material The online version of this article (https://doi.org/10.1007/s00477-018-1587-0) contains supplementary material, which is available to authorized users.

✉ Charles Onyutha
conyutha@gmail.com

[1] Faculty of Technoscience, Muni University, P.O Box 725, Arua, Uganda

Published online: 25 July 2018

2003; Nicholson 1996; Bunting et al. 1976). Actually, most of these studies tended to cover areas where observational rainfall data were available. Some studies on precipitation covering the entire African continent include Maidment et al. (2015), Kaptué et al. (2015), Giannini et al. (2008), Grimes et al. (2003), Nicholson (2001), Nicholson and Selato (2000), Nicholson (2000), Janowiak (1988), and Ogallo (1979). However, these studies were either based on short-term data periods for instance, 1983–2010 (Maidment et al. 2015), and 1998–2012 (Kaptué et al. 2015) or focused on analyses of only variability but not trends. Even those studies that analyzed trends never took into perspective the need to examine the variation in rising and falling short-durational trends (or sub-trends) that characterize fluctuations in the rainfall series. This might not be surprising because in detection of trends, it is a common practice that analyses are mainly conducted considering the long-term series as a whole (Onyutha 2016b). In fact, severe precipitation events tend to temporally occur in the form of clusters (above or below the long-term average) over certain data periods. This is a commonly blurred phenomenon to researchers interested in trend analyses. Eventually, the null hypothesis H_0 (no trend) may not be rejected at a selected α when the full time series is used as a whole yet if analyses are separately done over sub-periods, the H_0 can be rejected for a number of sub-trends.

Separating sub-trends over short-durations (e.g. of decadal time scales) from that of the long-term period (for instance due to global warming) makes it possible to attach physical explanations to the rising and falling trends within the given data. Besides, analyses of co-variation of precipitation and the possible driver (such as the large-scale ocean–atmosphere interactions), can be valuable in predicting an upcoming period of negative or positive sub-trend, something which is vital for planning of environmental management practices. The period over which significance of the sub-trend should be assessed depends on the cumulative effect of temporal variation in the variable. To do so, the author of this paper developed a method that employs both graphical and statistical techniques for analyses of trends and sub-trends (see Onyutha 2016b) as opposed to other common techniques (like the Mann–Kendall (MK) (Mann 1945; Kendall 1975) test) which purely rely on statistical results. Graphically, this method recently developed in Onyutha (2016b) separates sub-trends over unknown periods of increase or decrease in the given variable. However, for comparison of sub-trends, sub-periods can also be selected based on a universally clued-up decision of stakeholders. For instance, the baseline period 1961–1990 is widely used for climate studies. Therefore, sub-trend from this baseline can be compared with those from the data sub-periods before or after the period 1961–1990. This is vital to know whether the recent period has been wetter or drier than the past condition. However, for a reliable comparison, the sub-periods are required to be of reasonable length relevant for the intended application. For instance, a period of 30 years or more can be used to characterize climate fluctuations, 15-year data period is relevant for planning crop water requirements (Onyutha 2016a), water supply projects, or risk-based water resources applications, etc. To take into account temporal oscillations, the World Meteorological Organization [WMO] (2000) suggested that changes in climatic conditions be investigated using data of at least 50-year record length. In this study, for analyses of the overall trend in precipitation and comparison of results from sub-trends, data over record period longer than 50 years with high spatial resolution over the entire continent of Africa were required.

Some of the freely available rainfall products covering the entire continent of Africa include series from the Global Precipitation Climatology Centre (GPCC) (Meyer-Christoffer et al. 2011), Climatic Research Unit (CRU) (Harris et al. 2014), African Rainfall Climatology (ARC) (Novella and Thiaw 2013), Global Precipitation Climatology Project (GPCP) (Adler et al. 2003), Tropical Rainfall Measuring Mission (TRMM) (Huffman et al. 2007), Princeton global forcings (PGFs) (Sheffield et al. 2006), TAMSAT African Rainfall Climatology (Maidment et al. 2014), extended TAMSAT (Tarnavsky et al. 2014), etc. Some of these precipitation products (such as CRU, GPCC, and GPCP series) are obtained from gauge interpolations, while others (incuding PGFs, TRMM, and ARC) are hybrid data, that is, observational-reanalyses type or combined from satellite and ground-based measurements. A number of these rainfall products are of short-term period. For instance, although they cover till recent year, the series ARC, GPCP, TRMM, and PGFs started from 1983, 1979, 1998 (for TRMM) and 1948, respectively. However, some data such as CRU and GPCC cover long-term period 1901-to-present. Regarding freely available precipitation products over Africa, a "trade-off " always exists in selection of which series to use for analyses. Whereas precipitation of long-term period are coarse (monthly or annual) in temporal resolution, short-term data sets tend to be of high (daily or hourly) time scale. With respect to trend analyses, high-resolution hydro-meteorological data can be vital for non-stationary assessment of extreme events or wet and dry conditions (Onyutha 2017). However, in this study, there was a need to focus on trends and sub-trends in seasonal and annual precipitation based on long-term period (with reasonable length of sub-periods before and after the baseline period 1961–1990) while taking into perspective coverage, at high spatial resolution, of the entire African continent.

In precipitation trend detection, it is vital to analyze the significance of both trend direction and magnitude. This is because the H_0 (no trend) may not be rejected for the direction of a linear trend whose magnitude is so huge that it cannot be disregarded in decision making for management of environmental practices (Onyutha 2016a). Conversely, it remains possible that, even for a very small magnitude of linear trend (which may not be that important in practice), the H_0 (no trend) can be rejected when testing trend direction (Robson et al. 2000; Onyutha 2016a).

No any studies exist on analyses of trends and sub-trends in precipitation at a continental scale while testing the significance of both trend magnitudes and directions. Therefore, this study aimed at: (1) investigating precipitation trends and sub-trends across the entire Africa (2) testing the significance of both trend direction and the non-zero slope of a linear variation of precipitation with time, and (iii) investigating if the temporal variation in precipitation sub-trends could be explained by the changes in large-scale ocean–atmosphere conditions.

2 Data and methodology

2.1 Data

2.1.1 Precipitation

Monthly global precipitation of Harris et al. (2014) which initially was over the period 1901–2012 and later extended to run from 1901 to 2015 was obtained in gridded (0.5° × 0.5°) form via the link https://crudata.uea.ac.uk/cru/ (accessed: 18th June, 2017). The main strength of this extended data which is referred to as the Climatic Research Unit (CRU) Time-Series (TS) Version 4.0 (denoted as CRU TS4.0) is that it compiles station data of multiple variables from numerous sources into a consistent format (Climate Data Guide 2017). As a side note, the accuracy of the CRU-TS4.0 at a particular grid point depends on the number of surrounding weather stations used for the interpolation. The CRU-TS4.0 data set was based on analysis of over 4000 individual weather station records (Climate Data Guide 2017). However, the number of stations used to derive CRU-TS4.0 varied from one region to another. Many areas of the sub-Saharan Africa have low density of weather stations. Because of poor maintenance of data observation equipment, many weather stations are not continuously operational. Sometimes the operationality of the existing weather stations depends on the historical development and/or are interrupted by political turmoil. Eventually, the number of operational weather stations varied over time. Such data problems related to the distribution of weather stations (though not examined in this study) could influence the accuracy of results on precipitation trends (see Maidment et al. 2015; Washington et al. 2013). The variation in the number of stations over time could exaggerate variability in precipitation or bias in trend results. However, with respect to trend analyses, the CRU-TS data was found to be comparable with those from other well-known sources such as GPCC considering various periods 1901–2009, 1901–1950, and 1951–2009 (see Harris et al. 2014). Based on the information from the British Atmospheric Data Centre (BADC) online at http://badc.nerc.ac.uk (accessed: 17th June, 2014) and supplementary material provided by Harris et al. (2014), before producing the CRU-TS, thorough quality control is always done with respect to the update of archived data from various weather stations, in-filling of missing records, etc. (see Harris et al. 2014). Therefore, because it had long-term precipitation data at high spatial resolution, CRU-TS4.0 was used to obtain an insight into the changes in precipitation across the continent of Africa. However, because the number of stations influence the trend in the precipitation data obtained through interpolation, it is vital to note that spatial similarities of results should not be assessed at the level of individual point location but for larger areas.

Figure 1 shows the mean of precipitation over Africa considering long-term period 1901–2015. It can be noticed that the precipitation mean, especially of annual time scale (Fig. 1a) characterizes well the various climatic conditions across the continent (Fig. 1f). Countries shown in the map of Africa (Fig. 1f) were not labeled. However, names of the African countries can be consulted from the map in "Appendix A" following information from the Nations Online Project (NOP 2017). Long-term annual precipitation mean values between 1960 and 3086 mm were confined to areas around the gulf of Guinea especially over the coastal parts of Sierra Leone, Liberia, Cameroon and Gabon. Lowest mean values were obtained across the Sahara and Namib deserts (Fig. 1a). The long-term precipitation mean values for December–February (DJF), March–May (MAM), June–August (JJA), and September–November (SON) seasons can be seen in Fig. 1b–e. The lowest long-term seasonal precipitation values were also found along the Sahara desert (Fig. 1b–e). For the JJA precipitation, mean values below 100 mm were obtained below 5° N. The spatial distribution of the SON precipitation (Fig. 1e) was somewhat comparable to that of the annual time scale (Fig. 1a).

2.1.2 Climate indices

For an insight into the consequences, on variability in precipitation sub-trends, of pressure or temperature changes occurring over the different oceans, climate indices were used. The selected climate indices included the North Atlantic Oscillation (NAO) index (Jones et al. 1997),

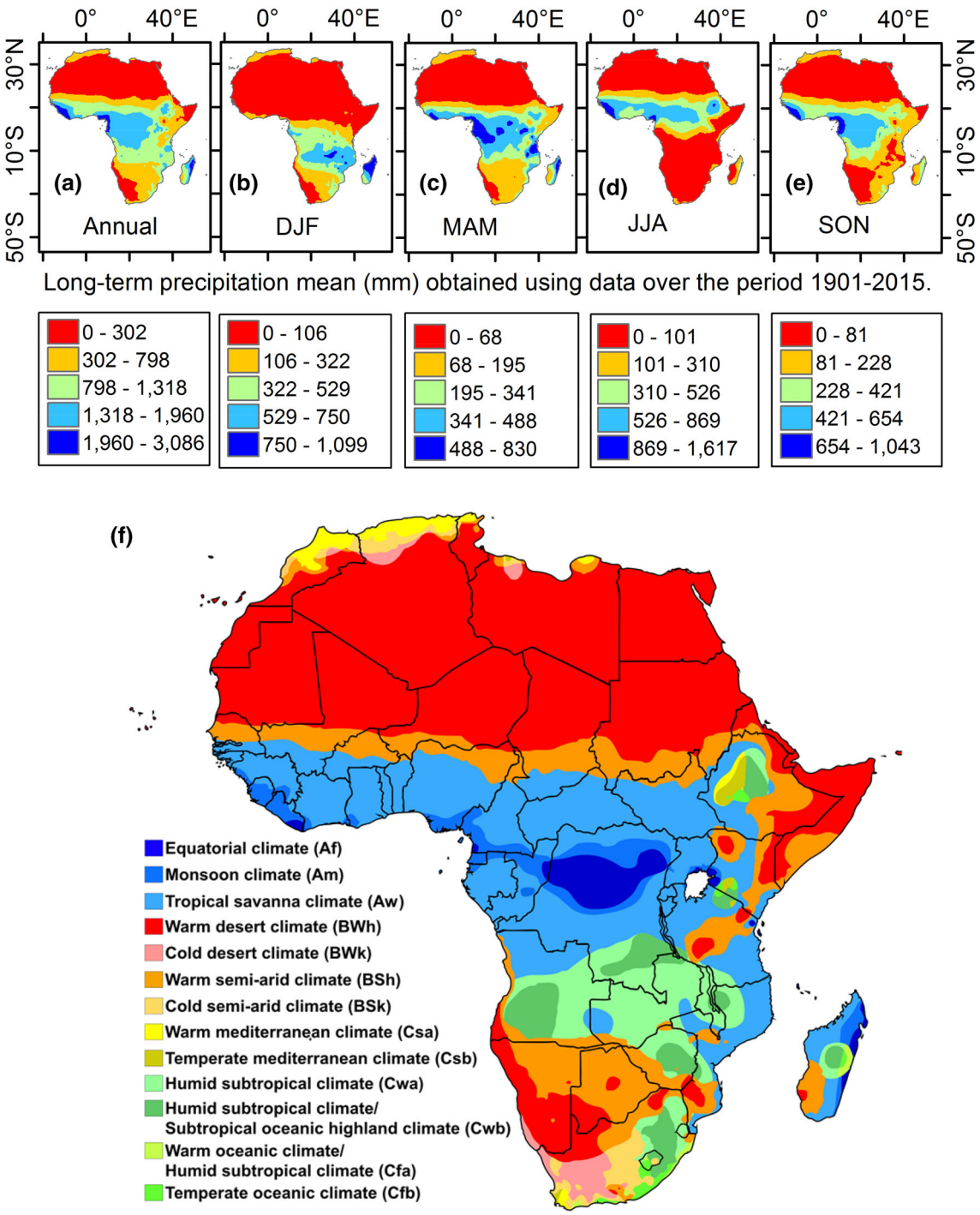

Fig. 1 Long-term precipitation mean (mm) of **a** annual and **b–e** seasonal time scales. Chart **f** shows the various climatic conditions across the African continent. (Source of chart **f**: ArcGIS 2017)

Atlantic Multidecadal Oscillation (AMO) index (van Oldenborgh et al. 2009), and Niño 3 index (Rayner et al. 2003; Trenberth 1997) and the Indian Ocean Dipole (IOD) index. The NAO index is the normalized Sea Level Pressure (SLP) difference between SW Iceland (Reykjavik), Gibraltar and Ponta Delgada (Azores). The IOD index can be defined as the anomalous Sea Surface Temperature (SST) difference between the western (50° E–70° E and 10° S–10° N) and the South Eastern (90° E–110° E and 10° S–0° N) Equatorial Indian Ocean. The AMO index refers to the SST averaged over 25° N–60° N, 7° W–70° W minus the regression on global mean temperature (van Oldenborgh et al. 2009). The AMO index was downloaded from the link http://climexp.knmi.nl/data/iamo_hadsst2.dat

(accessed: 29th January, 2013). The NAO index was downloaded online via the link http://www.esrl.noaa.gov/psd/gcos_wgsp/Timeseries/NAO/ (accessed: 16th April, 2016). The IOD index was obtained from the link http://www.jamstec.go.jp/frcgc/research/d1/iod (accessed: 20th January, 2014). Series for Niño3 was downloaded online via the link http://www.esrl.noaa.gov/psd/gcos_wgsp/Timeseries/Nino3/ (accessed: 29th January, 2013).

2.2 Long-term trend and sub-trends

In this study, analyses of both trend magnitudes and directions were considered. Trend magnitude (also referred to as the trend slope) expresses the amount by which the variable is expected to linearly change over a time unit of the observations (Onyutha 2017). On the other hand, trend direction is an indication of the dependence of the variable on time and this can be positively or negatively (Onyutha 2017).

2.2.1 Trend magnitude and its significance

The linear trend slope (m) can be computed using (Sen 1968; Theil 1950):

$$\mathrm{m} = Median\left(\frac{\mathrm{x_j}-\mathrm{x_i}}{\mathrm{j}-\mathrm{i}}\right), \quad \forall \mathrm{i} < j \tag{1}$$

To assess the significance of m from Eq. (1), the H_0 (trend magnitude is not time-dependent) i.e. H_0 ($m = 0$) and the alternative hypothesis H_1 ($m \neq 0$) can be tested at the selected α. This was done using the procedure adopted from Onyutha (2016c) where: The coefficient of the correlation between the data and the time of observations is first computed. Secondly, the data standard deviation and the computed correlation coefficient are used to calculate the standard error of the estimate. The statistic for testing the H_0 ($m = 0$) is computed as the ratio of m (Eq. 1) to the standard error of the estimate. The probability value (p value) based on Student's t–distribution is computed and compared with the selected α. If α is greater than or equal to the computed p value, the H_0 ($m = 0$) is rejected at α. In other words, if the computed p value $\leq \alpha$, H_1 ($m \neq 0$) is not rejected at α.

Using both seasonal and annual precipitation at each grid point, m (Eq. 1) was computed and its significance assessed by testing the H_0 ($m = 0$) at $\alpha = 0.05$. This was separately done for the periods 1901–2015, 1965–1990 and 1991–2015. To assess possible acceleration or deceleration of the precipitation increase or decrease, the Slope Difference (SD) was computed at each grid point by subtracting m (trend magnitude, mm/year) of the period 1991–2015 from that of 1965–1990. The period 1965–1990 was selected to characterize the past precipitation within the widely used baseline for climate studies. The period 1991–2015 was chosen to represent the recent climatic conditions.

2.2.2 Trend direction

Some methods, such as the MK (Mann 1945; Kendall 1975) test among others, exist for detection of long-term trends. However, since this study was about analyses of trends and sub-trends, the Cumulative Sum of rank Difference (CSD) method recently developed by Onyutha (2016a, b, c) was used. This method specifically deals with identification and analyses of trends and sub-trends in series. As already highlighted before, common methods (like the MK test) are purely statistical. In fact, Kundzewicz and Robson (2004) remarked that the use of purely statistical trend results can be meaningless sometimes. In the same vein, the CSD approach employs both graphical and statistical techniques for analyses of changes in series. The graphical component of the CSD approach is based on the pattern of the partial terms of the trend statistic that eventually is statistically used to test the H_0 (no trend) in the data (Onyutha 2016a, b, c). For detection of long-term trends, it was shown by Onyutha (2016a) that the statistical component of the CSD approach used in this study was comparable with the well-known MK test under various circumstances of sample sizes, variations, linear trend slopes, and serial correlations. Nevertheless, in this paper, trends in annual precipitation over the period 1901–2005 were detected using the CSD and MK tests and the spatial results across the African continent showing high comparability of the two approaches can be seen in Section 1.2 of the Supplementary Material. One important factor to consider for the choice of which method to use in this study was the huge number of precipitation series for analyses. Here, the CSD method was preferred to the MK test. This was because, the CSD approach quantifies the influence of data ties in a lumped way and this makes it computationally faster and appreciably simpler than considering groups of tied data points as done for the MK test (Onyutha 2016c). Furthermore, the CSD approach can be applied to analyze both trend and variability (something which is not the case for the common techniques meant purely for detecting long-term trends). The CSD trend analysis approach is implemented in a tool referred to as CSD-NAIM. This tool and its supporting documents can be freely downloaded online via the link: https://sites.google.com/site/conyutha/tools-to-download (accessed: 19 February 2018). The description of the CSD approach is given next.

For a given series X of sample size n, Y can be taken as the replica of X such that for $1 \leq i \leq n$, the ith transformed data point d_i can be obtained using (Onyutha 2016a, b, c):

$$d_i = 2\sum_{j=1}^{n} \mathrm{sgn}_1\left(y_j - x_i\right) - \left(n - \sum_{j=1}^{n} \mathrm{sgn}_2\left(y_j - x_i\right)\right) \quad (2)$$

where,

$$\mathrm{sgn}_1\left(y_j - x_i\right) = \begin{cases} 1 & \text{if } \left(y_j - x_i\right) > 0 \\ 0 & \text{if } \left(y_j - x_i\right) \le 0 \end{cases} \quad (3)$$

$$\mathrm{sgn}_2\left(y_j - x_i\right) = \begin{cases} 1 & \text{if } \left(y_j - x_i\right) = 0 \\ 0 & \text{if } \left(y_j - x_i\right) < 0 \text{ or } \left(y_j - x_i\right) > 0 \end{cases} \quad (4)$$

The rank difference d_i (Eq. 2) can be used to detect both trends and variability. Variability can be assessed by testing the null hypothesis H_0 (natural randomness) using the following procedure. Let β be the number of times when $d_{i-1} > 0$ and $d_i < 0$ for $2 \le i \le n$. Furthermore, consider γ as the number of times when $d_{i-1} < 0$ and $d_i > 0$ for $2 \le i \le n$. We can make $\Omega = \beta + \gamma$. The distribution of Ω is approximately normal with the mean and variance given by $[2^{-1} \times (n-1)]$ and $[4^{-1} \times (n-1)]$, respectively. If the probability (p) value computed using the z-statistic given by $[(n-1)^{-0.5} \times |(1-n+2\Omega)|]$ is less than or equal to the selected significance level, the H_0 is rejected; otherwise, the H_0 is not rejected.

Trend can be tested using d_i (Eq. 2) both graphically and statistically. To make graphical diagnosis of the change in the series, the cumulative sum S_i of the rank difference d_i (Eq. 2) can be obtained using

$$S_i = \sum_{j=1}^{i} d_j \quad \text{for } 1 \le \mathrm{i} \le \mathrm{n} \quad (5)$$

and the CSD plot (i.e. a plot of S_i (Eq. 5) against the time of the observations for instance, data years for annual series) can be used to make graphical diagnosis of changes in the series. For a time series characterized by a positive (negative) trend, the entire (or most part of the) CSD plot forms a curve above (below) the $S_i = 0$ line which can be taken as the reference. If there is no trend in the series, the scatter points in the CSD plot cross the reference in a random way. Further information on the effect of data transformation using Eq. (2) and an illustration of how to use the CSD plot based on Eq. (5) to diagnose changes in the given series can be found in Section 1.1.1 of the Supplementary Material.

Statistically, the CSD trend statistic T can be computed using (Onyutha 2016b):

$$T = \frac{6}{(n^3 - n)} \sum_{i=1}^{n-1} S_i \quad (6)$$

where S_i is from Eq. (5).

Positive and negative trends are indicated by $T > 0$, and $T < 0$, respectively. The standardized trend test statistic Z which follows the standard normal distribution with mean (variance) of zero (one) is computed using Eq (7). Consider $Z_{\alpha/2}$ as the standard normal variate at the selected α, the H_0 (no trend) is rejected if $|Z| \ge Z_{\alpha/2}$, otherwise, the H_0 is not rejected. While taking into account the required correction of V (i.e. variance of T) from the influence of persistent fluctuations in the series, Z can be computed using (Onyutha 2016a, c):

$$Z = \frac{T}{\sqrt{V}} \quad (7)$$

where,

$$V = \frac{1}{n-1}\left(1 - \frac{10}{17}e^2 - \frac{7}{17}e\right) \times \left|1 + \frac{2}{n(n^2-3)} \times \sum_{k=1}^{n-2} (n-k)^3 r_k^{\alpha}\right| \quad (8)$$

while, e as the measure of ties is given by

$$e = \frac{-1}{n^2 - n}\left(n - \sum_{i=1}^{n}\sum_{j=1}^{n} \mathrm{sgn}_2\left(y_j - x_i\right)\right) \quad (9)$$

and $\mathrm{r_k^{\alpha}}$ as the lag-k correlation coefficient (r_k) significant at α. Before computing r_k, the linear trend slope (m) is computed using Eq. (1). Next, for $1 \le i \le n$, detrended series C is obtained by $C_i = X_i - m \times i$. Let $\mathrm{C^{\#}}$ be the mean of the C_i's, the values of the r_k can be computed using Eq. (10) (Salas et al. 1980) and the 100(1 − α) % confidence interval limits (CI_{lim}) for testing the significance of r_k (i.e. to determine $\mathrm{r_k^{\alpha}}$) can be obtained using Eq. (11) (Anderson 1941):

$$r_k = \frac{\frac{1}{(n-k)}\sum_{i=1}^{n-k}\left(C_i - C^{\#}\right)\left(C_{i+k} - C^{\#}\right)}{\frac{1}{n}\sum_{i=1}^{n}\left(C_i - C^{\#}\right)^2} \quad (10)$$

$$\mathrm{CI_{lim}} = \frac{-1 \pm \mathrm{Z}_{\alpha/2}\sqrt{\mathrm{n-k-1}}}{\mathrm{n}-k} \quad (11)$$

and in Eqs. (10)–(11), k should be set to vary from $k = 1$ up to $n - 2$ (see Onyutha 2016a).

Using both seasonal and annual precipitation at each grid point, trend directional statistic Z (Eq. 7) was computed and its significance assessed by testing the H_0 (no trend) at $\alpha = 0.05$. This was separately assessed over the periods 1901–2015, 1965–1990 and 1991–2015.

2.2.3 Correlation between precipitation sub-trends and climate indices

To assess temporal variation in the sub-trends, a relevant time scale t can be selected. For instance, to assess the influence of decadal oscillations, t = 10 years can be chosen. To characterize climate fluctuations, the window length t can be set to about 30 years. If a time scale of 35 years is selected for series with data years 1901, 1902,…, 2015, the sub-series can be extracted from the window moved each time by a unit over the sub-periods 1901–1935, 1902–1936,…, and 1981–2015, respectively. To each sub-series, Eq. (7) is separately applied. To ensure no loss of information at the beginning and end of the series, a general framework can be adopted to ensure the number of the sub-series equals n.

If X comprises a subset x from the qth to the uth value of X, Eq. (7) can be applied based on a window moved in an overlapping way from the beginning to the end of the series. In other words, if for the selected or chosen t, $w = 0.5 \times (t + 1)$ and $w = 0.5 \times t$ in the cases when t is odd and even respectively,

$$Z_j^{(t)} = f\left(x \subset X | x_q \leq x \leq x_u\right) \quad \text{for } j=1, 2, \ldots, n \tag{12}$$

where Z_j is the jth value of Z, and the terms q and u are all based on j and can be given by:

$$\left.\begin{array}{l} \text{if } j < w, \quad q = 1, \quad u = t + j - w - 1 \\ \text{if } j \geq w \text{ and } j \leq (n - w), \quad q = j - w + 1, \quad u = j + w \\ \text{if } j > (n - w) \text{ and } j \leq n, \quad q = j - w + 1, \quad u = n \end{array}\right\} \tag{13}$$

To test the H_0 (natural randomness), thresholds on the variability can be constructed using $\pm Z_{\alpha/2}$ after plotting Z_j against the corresponding jth data year. An illustration of the temporal variation for various time scales can be found in Section 1.1.3 of the Supplementary Material. The code for analysis of temporal variability using CSD approach, for instance based on Eqs. (12, 13), is implemented in a CSD-based Variability Analyses Tool called CSD-VAT. This tool and its supporting document can be freely downloaded online via the link: https://sites.google.com/site/conyutha/tools-to-download (accessed: 18 July 2018).

Possible linkage of the variation in precipitation sub-trends to changes in large-scale ocean–atmosphere conditions was sought in terms of the correlation analysis. Firstly, sub-trends were computed (using 15-year time scale) from both precipitation (at each grid point) and climate indices. The monthly climate indices were initially converted to seasonal and annual time scales as considered for the gridded precipitation. Secondly, the H_0 (no correlation between the sub-trends of precipitation and those of the climate indices) was tested at α = 0.01 (at each grid point).

3 Results and discussion

3.1 Trends and sub-trends

Figure 2 shows results of statistical analyses of long-term trends and sub-trends. For the period 1901–2015, the ranges of trend slopes were narrower for annual (Fig. 2a) than those of seasonal precipitation (Fig. 2b–e). Most parts of Africa especially North of 10° N were characterized by a decrease in precipitation. The largest precipitation decrease (at a rate of about − 3.0 mm/year) was found in West Africa especially over Senegal, Guinea, Sierra Leone, Liberia, the Southern part of Nigeria and Western Cameroon (for annual precipitation), Senegal, Guinea Bissau, and Gambia (for JJA and SON season). For annual and SON precipitation (Fig. 2a, e), the largest increase in precipitation was obtained over Gabon, Southern part of Congo, North Western area of Angola, and the Equatorial region around Lake Victoria in East Africa. In the Western part of the Southern Africa, increasing trend was found in annual, DJF, MAM and SON precipitation (Fig. 2a–c, e). This is consistent with the results from a recent study by Kruger and Nxumalo (2017) in which the precipitation from 1921 to 2015 especially over the West of South Africa was characterized by an increase. The season for which most parts of Africa exhibited a decrease in precipitation was JJA, followed by MAM, DJF and finally SON. The MAM precipitation over the Namib desert was characterized by an increase (Fig. 2c). Generally, the ranges of trend slopes in the precipitation from 1901 to 2015 (Fig. 2a–e) were wider than those for the periods 1961-1990 (Fig. 2f–j) and 1991–2015 (Fig. 2k–o).

For the period 1961–1990 (Fig. 2f–j), the precipitation across the Sahara desert or areas North of 10° N was characterized by a decrease. For annual time scale (Fig. 2f), it is noticeable that precipitation decrease by magnitude more than 5 mm/year was mainly along 10° N. In the areas south of 10° S, the precipitation was mostly characterized by an increase especially for the DJF, MAM and SON seasons (Fig. 2g–h, j). An increase by more than 5 mm/year was noted for the SON precipitation (Fig. 2j) in West Africa over Liberia, Sierra Leone, and Guinea) as well as in East Africa especially around the Ethiopian Highlands. For the DJF precipitation, an increase of more than 5 mm/year was found in Madagascar, and Southern Angola (Fig. 2g). Along the Sahel region, there was a decrease in the DJF, MAM, JJA and annual precipitation (Fig. 2g–i).

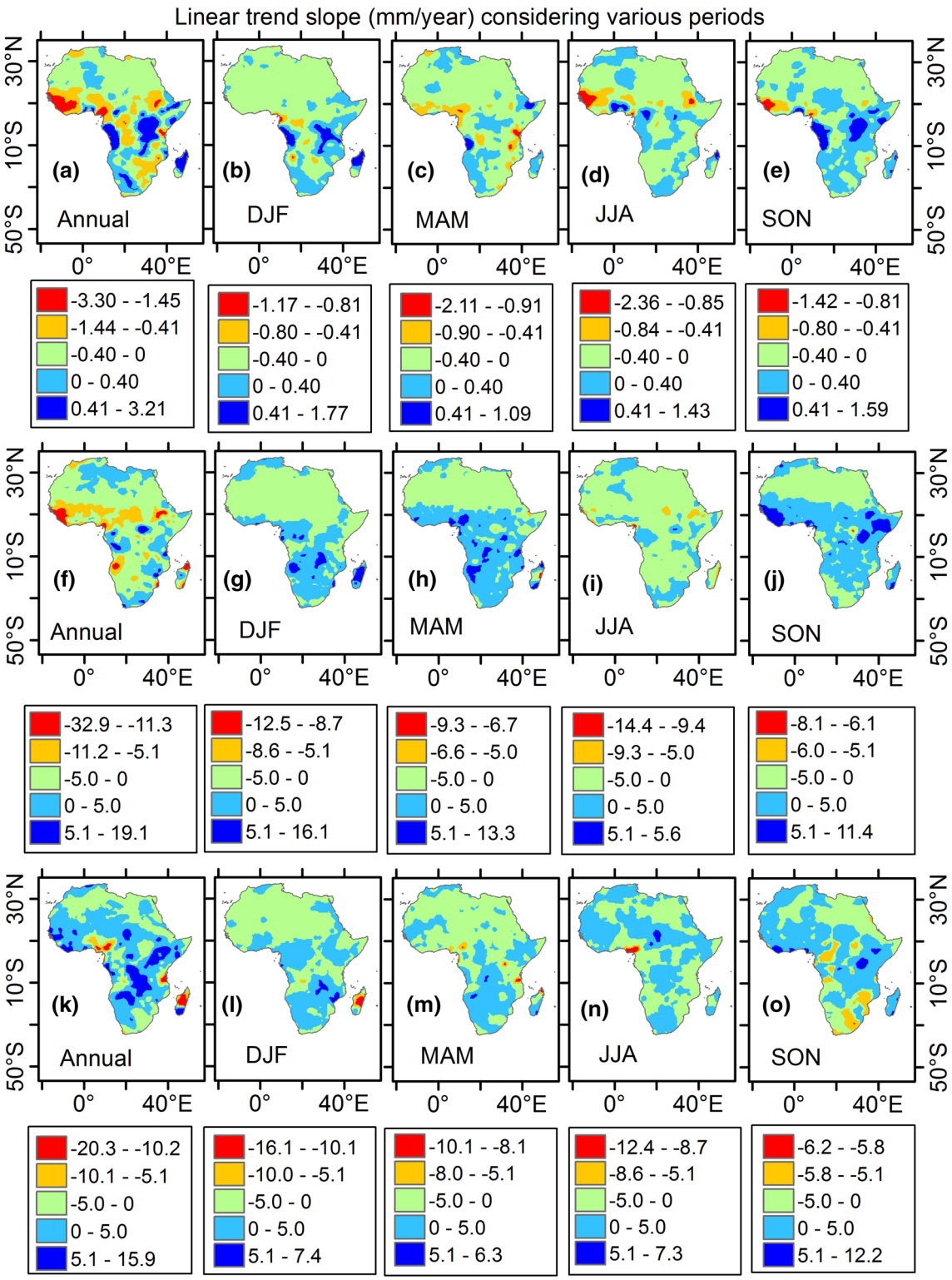

Fig. 2 Linear trend magnitude (mm/year) for the period **a–e** 1901–2015, **f–j** 1965–1990, and **k–o** 1991–2015

For the period 1991–2015, annual precipitation increased in most parts of the African continent (Fig. 2k). An increase in annual precipitation by greater than 5 mm/year was found in the North Eastern Angola, and the Great Lakes region of the Equatorial area. Decrease of magnitude greater than 5 mm/year was exhibited by annual precipitation in the Northern Madagascar, South of Nigeria and North Western Cameroon. Over most parts of Africa,

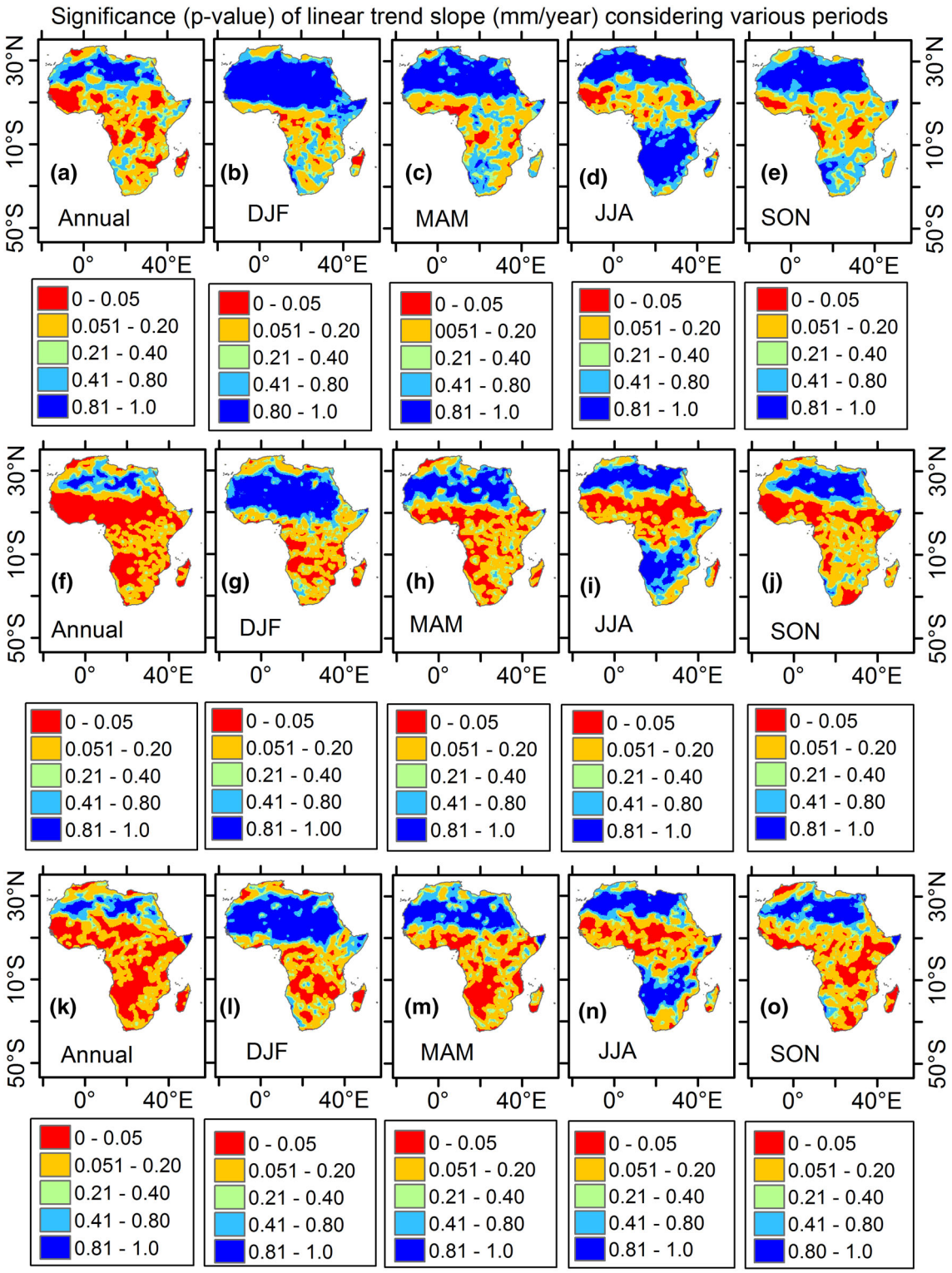

Fig. 3 Probability (p value) of the linear trend slope for the period **a–e** 1901–2015, **f–j** 1965–1990, and **k–o** 1991–2015. The p values less or equal to 0.05 show locations where the H_0 ($m = 0$) was rejected at $\alpha = 0.05$

annual precipitation exhibited a decrease over the period 1961–1990 (Fig. 2f) and an increase for the 1991–2015 (Fig. 2k). For the area North of 10° N, DJF and MAM precipitation was mainly characterized by a decrease. Along the Sahel region, there was an increase in the JJA and SON precipitation. In the Southern Africa,

precipitation exhibited a decrease (an increase) in the SON (DJF or MAM) season (Fig. 2g–h, i).

Figure 3 shows the significance of precipitation trend magnitudes. In the legends of Fig. 3a–o), the p values less or equal to 0.05 show locations where the H_0 ($m = 0$) was rejected ($p < 0.05$). Over the period 1901–2015, the H_0 ($m = 0$) was rejected ($p < 0.05$) for: (1) the precipitation decrease over West Africa especially in Ivory Coast, Guinea, Sierra Leone, Liberia, Senegal and South Mali (Fig. 3 a) (2) an increase in annual and SON precipitation around the Lake Victoria in East Africa, as well as over Gabon and Southern part of Congo (Fig. 3a, e), (3) DJF season (around Lake Victoria), for MAM season (Southern Nigeria and Western Cameroon), and JJA precipitation (Senegal and South Mali) (Fig. 3b–d).

For the period 1961–1990, the H_0 ($m = 0$) was rejected ($p < 0.05$) for: (1) the annual, MAM, JJA and SON precipitation along the 10° N, and (2) the decrease in annual precipitation South of 10° S especially over South Angola and North Namibia (Fig. 3g). For the period 1991–2015, the H_0 ($m = 0$) was rejected ($p < 0.05$) for the increase in SON precipitation around the Lake Victoria or the Horn of Africa (Fig. 3o). Furthermore, the H_0 ($m = 0$) was rejected ($p < 0.05$) for the increase in: (1) annual precipitation in the North Eastern Angola, and the Great Lakes region of the Equatorial Africa, and (2) MAM precipitation over South Angola (Fig. 3m).

Figure 4 shows the significance of trend directions in annual and seasonal precipitation over the periods 1901–2015, 1965–1990, and 1991–2015. Over the period 1901–2015, the H_0 (no trend) was rejected ($p < 0.05$) for: (1) precipitation decrease in a number of areas including West Africa (Senegal, Guinea, Sierra Leone, Liberia, Southern part of Nigeria), and Egypt (Fig. 4a–e), (2) an increase in annual and SON precipitation over Gabon, Southern part of Congo, and the Equatorial region around Lake Victoria in East Africa (see Fig. 4a, e), and (3) an increase in JJA precipitation over North Western Angola and South Eastern part of the Democratic Republic of Congo (Fig. 4c).

For the period 1965–1991 (Fig. 4f–j), the H_0 (no trend) was not rejected ($p > 0.05$) in most parts of the continent for both annual and seasonal precipitation. The positive and negative directional trend signs were more mixed for annual precipitation than those of seasonal time scales (Fig. 4a–e). In the same vein, Omondi et al. (2014) also found for the Greater Horn of Africa that, the trends in the annual precipitation using data from 1961 to 2010 were both mixed up in directions and even mostly insignificant. However considering the entire Africa, the H_0 (no trend) was rejected ($p < 0.05$) over the North Western Namibia, and some Western African countries including Guinea, and Ivory coast (for annual precipitation, Fig. 4f), and North Western part of Libya (for DJF precipitation, Fig. 4g). For both seasonal and annual precipitation, there were more areas where the H_0 (no trend) was rejected ($p < 0.05$) over the period 1991–2015 than those for 1965–1990. For the period 1991–2015, the notable areas where the H_0 (no trend) was rejected ($p < 0.05$) include the Sahel region (for annual and JJA precipitation, Fig. 4k, n), Namibia (for MAM precipitation, Fig. 4m), North Eastern Cameroon and South Western Chad (for DJF precipitation, Fig. 4l), and Southern Ethiopia (for SON precipitation, Fig. 4o).

Figure 5 shows statistical results from further analyses of sub-trends in terms of the Slope Difference (SD, mm/year). For clarification on the interpretation of SD values, let mA and mB denote m (Eq. 1) of the periods 1965–1990 and 1991–2015, respectively. SD would be positive if: (i) $m_A < 0$ and $m_B < 0$ but $|m_A| < |m_B|$, (ii) $m_A > 0$ and $m_B < 0$, (iii) $m_A > 0$ and $m_B > 0$ but $|m_A| > |m_B|$. However, SD would be negative if: (i) $m_A > 0$ and $m_B > 0$ but $|m_A| < |m_B|$, (ii) $m_A < 0$ and $m_B > 0$, (iii) $m_A < 0$ and $m_B < 0$ but $|m_A| < |m_B|$. For both annual and seasonal precipitation, low SD values in the range -1 to 1 mm/year were obtained in areas north of 10° N (Fig. 5a–e). For JJA precipitation (Fig. 5d), low SD values in the range -1 to 1 mm/year were mainly south of the Equator. However, positive SD values greater than 1 mm/year for the JJA precipitation were mainly in the Sahel belt (Fig. 5d). This increase in precipitation especially during the peak monsoon (JJA) indicated the recovery of the Sahel region from dry conditions in the 1970s and 1980s (Brandt et al. 2014; Maidment et al. 2015). An increase in the recent precipitation over the Sahel region could be attributed to the low-frequency variability linked to the Interdecadal Pacific Oscillation (Villamayor and Mohino 2015). However, other influencing factors, as reported by Maidment et al. (2015) could be the changing concentrations of Northern Hemispheric anthropogenic aerosols (Dong et al. 2014), and amplification of the Saharan heat low by the greenhouse gas-induced warming (Dong and Sutton 2015).

In the Eastern Africa (around the Ethiopian Highlands, or the Horn of Africa) and the West African region south of the Sahel belt, SD values were positive for the SON precipitation (Fig. 5e). Over the Horn of Africa, it is noticeable that the SON precipitation (Fig. 5e) was characterized by positive SD values (around 6 mm/year). This finding agrees with the results from recent studies (Liebmann et al. 2014; Rowell et al. 2015) which showed that the October–December season has recently become wetter than the past. The SD of the annual precipitation (Fig. 5a) characterized the net effect of the changes in the trend magnitudes from the various seasonal time scales (Fig. 5b–e). Around the Equator, some areas such as Gabon and the Republic of the Congo experienced negative SD values of about $-$ 10 mm/year for annual precipitation (and DJF season to some

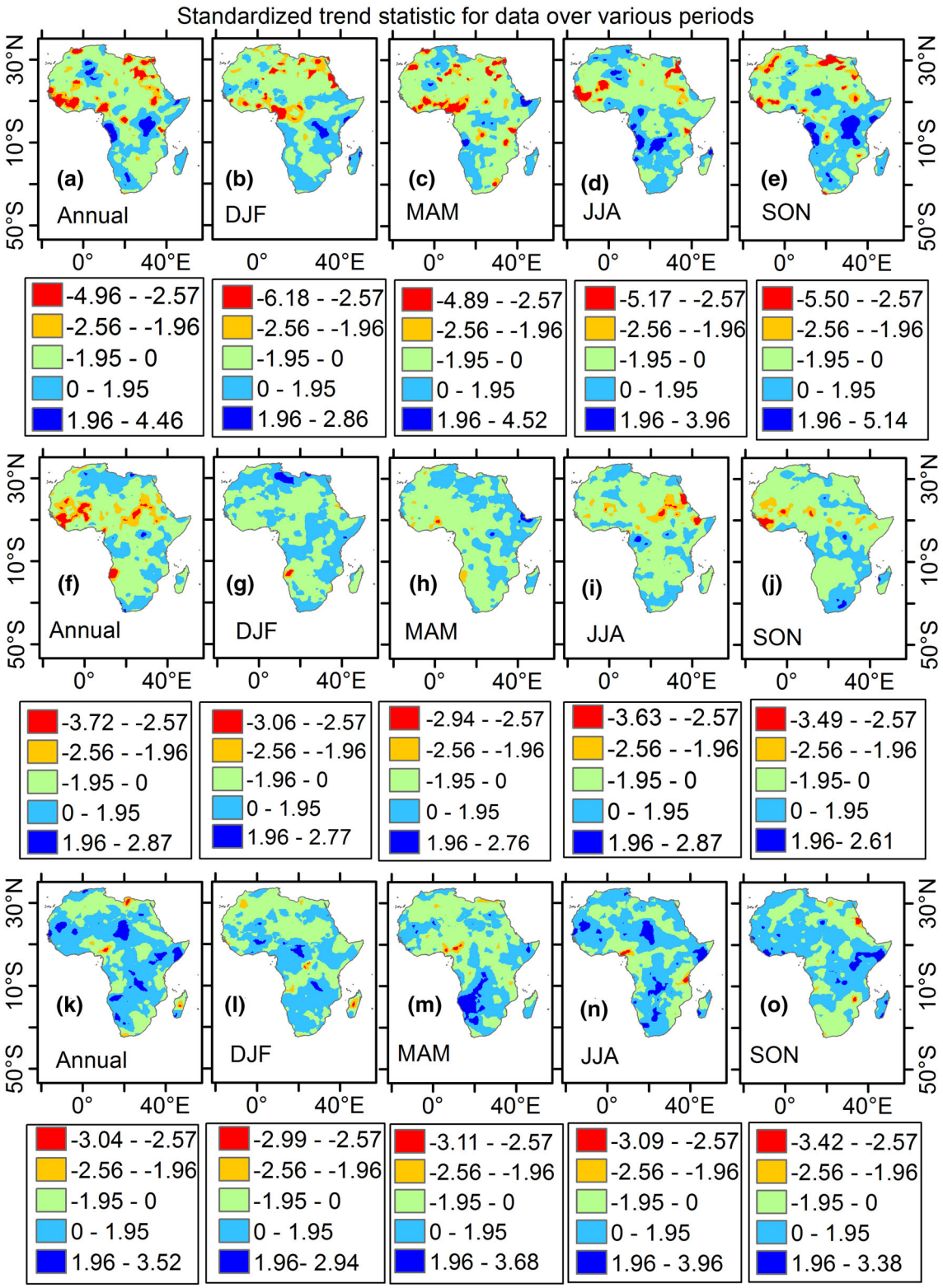

Fig. 4 Standardized trend statistic Z for the period **a–e** 1901–2015, **f–j** 1965–1990, and **k–o** 1991–2015. The values $Z = 1.96$ and 2.57 are the thresholds for rejecting the H_0 (no trend) at $\alpha = 0.05$ and 0.01, respectively

extent). This was consistent with the finding from Diem et al. (2014). Using ARC data, Diem et al. (2014) showed that this recent (1983–2012) significant drying for the Central Equatorial Africa was highly correlated with the

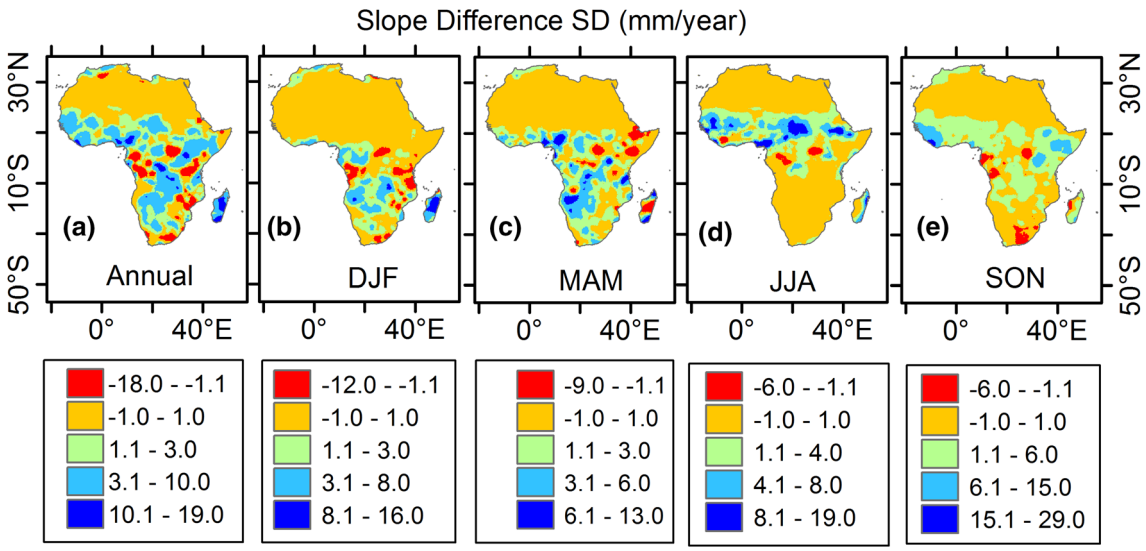

Fig. 5 Slope Difference (SD) in terms of trend magnitude (mm/year) based on the period 1965–1990 minus that of 1991–2015 for **a** annual, **b** DJF, **c** MAM, **d** JJA and **e** SON precipitation

index of SST centered on the North Atlantic Ocean also referred as the Atlantic Multidecadal Oscillation (AMO). For the DJF precipitation, noticeable changes in the trend slopes were obtained for areas south of the latitude 5° N (Fig. 5b). For the MAM precipitation (Fig. 5c), large positive SD values were obtained in the North Western Namibia, South Western Angola, Cameroon and Southern Nigeria. However, negative SD values were obtained in the Horn of Africa. This is consistent with the well-known recent decrease in the precipitation over the Horn of Africa (Rowell et al. 2015). Although this decline in the MAM precipitation (especially over the Horn of Africa) may be attributed to internal climate variability, Tierney et al. (2015) asserted that it is synchronous with the recent regional and/or global warming, and thus the possible linkage to the anthropogenic factor.

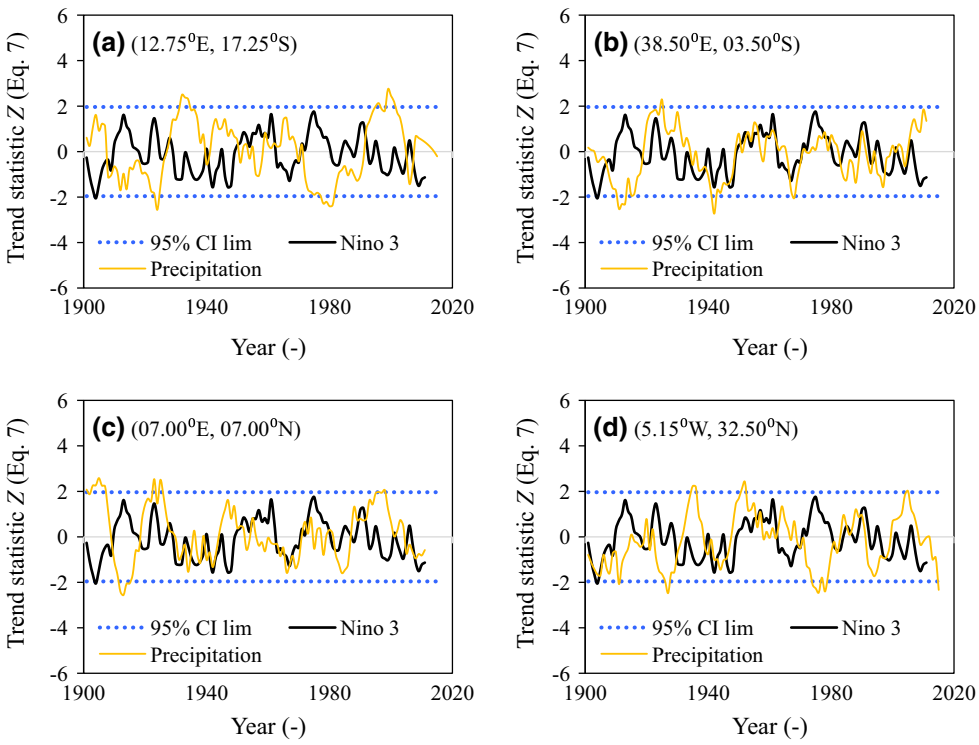

Fig. 6 Comparison of the variation in 15-year sub-trends from the Niño 3 and annual precipitation over the **a**, **b** Southern hemisphere, and **c**, **d** Northern hemisphere based on series extracted at selected coordinates shown in "()". In the legend, "CI lim" stands for confidence interval limits

3.2 Correlation between precipitation variability and climate indices

Figure 6 shows, for illustration, the temporal variability in annual precipitation along with Niño 3. To obtain Fig. 6, annual precipitation was obtained at four selected locations the coordinates of which can be seen in the labels of each chart. It is noticeable that over some sub-periods, the values of Z were consecutively positive or negative. This depicts an oscillatory behavior of precipitation over multi-decadal time scales. Thus, the values of the trend statistic Z (Eq. 7) consecutively above or below the reference (i.e. $Z = 0$ line) characterized oscillation highs and lows respectively. This gives information on the occurrence of precipitation wet and dry conditions in a clustered way in time. Since the 95% confidence interval limits were up- or down crossed by the sub-trends, the H_0 (natural randomness) was rejected ($p < 0.05$) for all the selected locations. The percentage of variance in the sub-trends that could be explained by Niño 3 varied from one location to another such as 32.4, 2.32, 2.25, and 0.52% at the coordinate points (12.75° E, 17.25° S), (38.50° E, 03.50° S), (07.00° E, 07.00° N), and (for 05.15° W, 32.50° N), respectively (see Fig. 6a–d). This suggests that the variation in precipitation across the various regions may be explained by changes in different possible predictors (e.g. Niño 3). The results of correlation between the variation in annual precipitation across the African continent and the selected climate indices (as illustrated in Fig. 6) can be seen next in the form of maps.

Figure 7 shows the spatial distribution of the coefficient of correlation between variability in the precipitation and climate indices. The amount of variance in the precipitation sub-trends that could be explained by the climate indices went up to 42, 44, 50, and 36% for IOD (Fig. 7c), AMO (Fig. 7j), NAO (Fig. 7m), and Nino 3 (Fig. 7p, r), respectively. For the correlation coefficient of magnitude greater than 0.25, the H_0 (no correlation between precipitation and climate indices) was rejected ($p < 0.01$). Because, the changes in large-scale ocean–atmosphere conditions explain variability in precipitation of a heterogeneous area more suitably at a regional than location-specific scale (Onyutha and Willems 2017a), it is vital that the results such as those from Fig. 7a–t be assessed at a regional spatial scale.

Along the Sahel region, positive correlation was found between AMO and precipitation of JJA (Fig. 7g), SON (Fig. 7h) and annual (Fig. 7j) time scales. It was previously shown by Nicholson (2000) that the precipitation over the Sahel region is influenced by changes in the SST from the Equatorial Atlantic and Indian Oceans. Considering the East African region, positive correlation (significant, $p < 0.01$) was found IOD and SON precipitation (Fig. 7c). SON precipitation over Madagascar was positively correlated (in a significant way at $\alpha = 0.01$) to NAO (Fig. 7 m). Around the Lake Victoria, negative correlation (significant, $p < 0.01$) was also found between NAO and the DJF precipitation (Fig. 7n). The Niño 3 was positively correlated (in a significant way at $\alpha = 0.01$) with JJA and annual time scales precipitation around Somalia (Fig. 7q, t). These results show that, other than the influence from the Indian Ocean, the variability of the East African precipitation is also linked to the changes in the SLP over the Pacific and Atlantic Oceans. Even using the SST, Balas et al. (2007) also showed that the precipitation variability in the West Central Africa is influenced by forces from the Pacific, Atlantic and Indian Oceans. The variation in the SST from the Indian Ocean influences the East African precipitation variability by altering the local Walker circulation (Tierney et al. 2013). Some of the past studies that found influences from the Atlantic Ocean (in terms of changes in SST) on the variability of Western and Central parts of the Equatorial Africa include Zhang and Delworth (2006) and Onyutha and Willems (2015; 2017b). Several studies (see for instance, Lyon and DeWitt 2012; Williams and Funk 2011; Onyutha and Willems 2015) showed that the precipitation over East Africa is driven by changes SLP or SST over the Pacific Ocean. However, other studies (such as Nicholson 2015; Liebmann et al. 2014; Tierney et al. 2013; Bergonzini et al. 2004) maintained that more influential forces that drive East African precipitation come from the Indian Ocean than those from the Pacific Ocean.

Considering the Southern Africa, MAM precipitation was positively correlated (significantly, $p < 0.01$) with IOD (Fig. 7a). It was shown by Washington and Preston (2006) that the Indian Ocean SST influences the variability of the South African precipitation. Negative correlation (significant, $p < 0.01$) was found between NAO and MAM (Fig. 7k). However, SON precipitation (Fig. 7m) was positively (in a significant way, $p < 0.01$) correlated with NAO (Fig. 7m). Furthermore, negative correlation (significant, $p < 0.01$) was also found between Niño 3 and the precipitation of DJF (Fig. 7s) and annual (NAN) (Fig. 7t) time scales. The variation in the SST in the Equatorial Pacific Ocean (or the El Nino Southern Oscillation i.e. ENSO) was also found in past studies (Lindesay 1988; Reason et al. 2000; Landman and Beraki 2012) to influence South African rainfall.

Over West Africa, MAM precipitation over was negatively correlated with NAO (Fig. 7k). However, JJA, SON and annual precipitation was significantly ($p < 0.01$) correlated with AMO (Fig. 7g, h, j). Variability of the West African precipitation is known to be linked to driving forces (e.g. SST variation) from the Tropical Atlantic Ocean (Ta et al. 2016). Positive significant ($p < 0.01$)

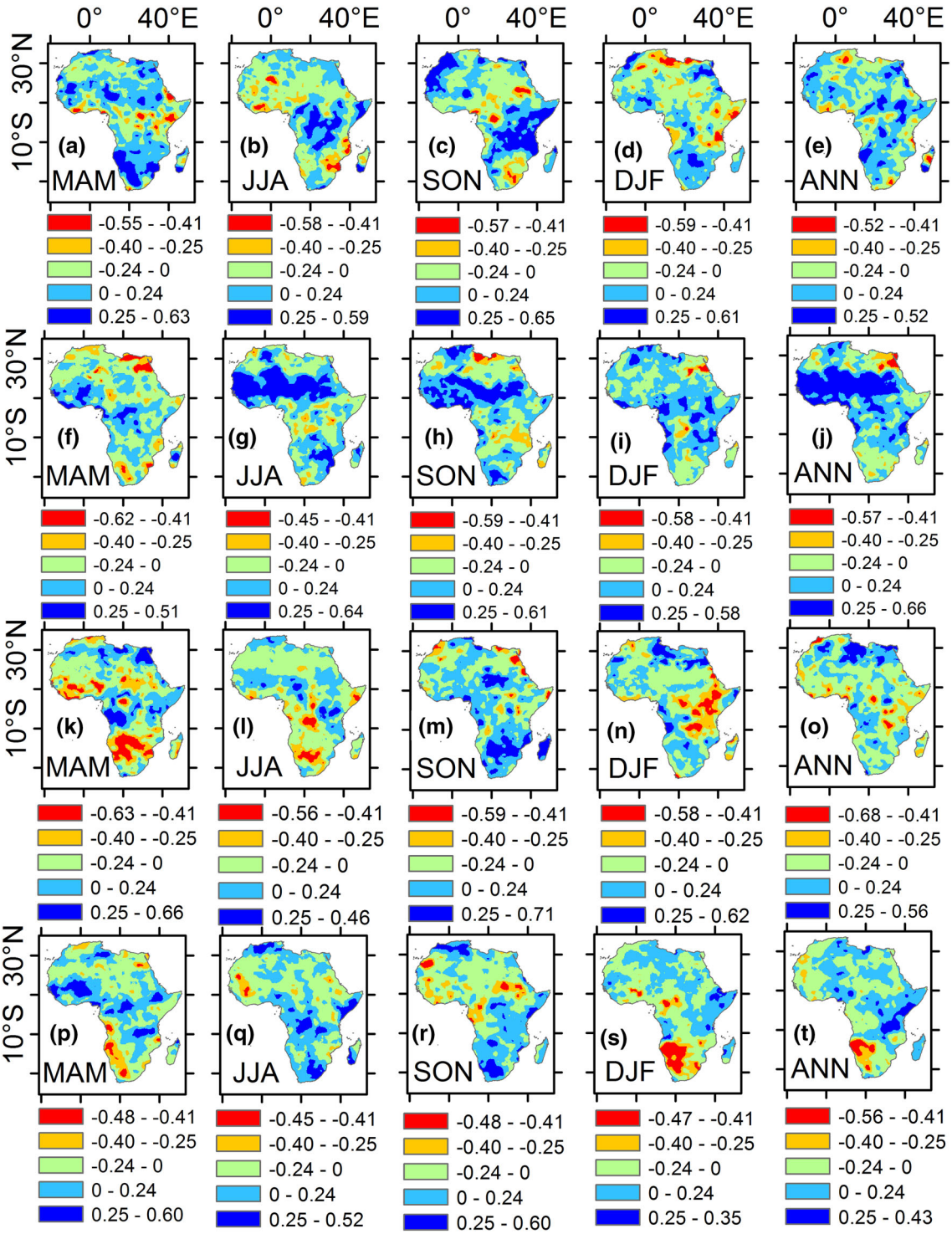

Fig. 7 Correlation between precipitation and **a–e** IOD, **f–j** AMO, **k–o** NAO, and **p–t** Niño 3 based on annual (ANN) and seasonal (MAM, JJA, SON, and DJF) time scales. The critical value for rejecting H_0 (no correlation) at $\alpha = 0.01$ is 0.25

correlation was obtained between Niño 3 and precipitation of MAM (Fig. 7p) and SON (Fig. 7r) time scales. However, Niño 3 was negatively correlated with DJF precipitation (Fig. 7s). A study by Rowell et al. (1995) also revealed that the variability of West African precipitation is influenced by ENSO.

3.3 Discussion

In trend analyses, significance of trend direction and magnitude is crucial for decision making by environmental management practitioners. Considering a long-term period 1901–2015, the significance of precipitation trends over certain regions of Africa poses serious concern for future management of water resources and agricultural practices. For regions characterized by decreasing (increasing) precipitation, if such a trend continues into the future, something which may be likely under the on-going global warming (Intergovernmental Panel on Climate Change IPCC 2007), it means dry (wet) areas will become drier (wetter) than the past condition. It can be possible that such a persistent trend (together with climate variability) may even alter the frequency and severity of future extreme precipitation conditions from their expected normal occurrences. Therefore, given the possible complexity in management of applications or practices related to precipitation under future climatic conditions, there should be a careful planning of possible adaptation measures. For instance, instead of the conventional assumption of stationarity of precipitation extreme events in determining hydro-meteorological quantiles, flood and drought return levels can be obtained using non-stationary frequency analyses in which the deterministic function of time is considered (see e.g. Onyutha 2017).

The results on SD at a particular location give an insight on whether the place is becoming wetter or drier than the past condition something which has implications for subsistence of the local population. For instance, over areas such as Somalia in the Horn of Africa where MAM season has the "long rains", a decreasing trend in the MAM precipitation signals an alarming possibility of persistent dry conditions. Given the existing vulnerability of the Horn of Africa, further decrease in precipitation will increase the food insecurity under future climatic conditions. For possible adaptation measures to the effects of the changes in precipitation on agriculture, cautious planning is required with respect to future crop water requirements. Suitable scientifically improved crop varieties which are drought-tolerant can be identified for the smallholder farming. Regarding variability of precipitation sub-trends, note can be taken that wet and dry conditions tend to occur in clusters. The frequency of precipitation events over wet and dry periods can differ. Therefore, planning and design of applications which depend on precipitation should be in a more considerate way than if wet and dry conditions would occur fully randomly on a year-to-year basis. Besides, when a suitable driver of precipitation variability is known, it becomes possible to predict an upcoming epoch of wet or dry conditions.

Based on the findings regarding the correlation between the variation in precipitation sub-trends and climate indices, there are two points to take into consideration. Firstly, the driving forces from the various oceans may influence one another in how they shape precipitation distribution across Africa. For instance, for transmission of the driving forces from the Pacific Ocean (think about the ENSO signal), the requirement of zonal circulation over the Indian Ocean is critical (see Goddard and Graham 1999). The second note is that the strength of the driving force from each ocean in influencing precipitation over a given region can vary over time. The Indian Walker cell can be weak over one period and strong during another (Nicholson 2017). For the corresponding periods, there can also be changes in strength of the descending or ascending poles of the Atlantic or Pacific cell (Nicholson 2017). Therefore, it remains possible that the strength (as well as the directional signs whether negative or positive) of the force driving precipitation variability over a region may depend on the period and/season considered for analyses (Onyutha and Willems 2017a; Onyutha et al. 2016). In other words, over one period, a particular force can drive precipitation variability in a positive way while for another period the influence is directionally negative. If a long-term period e.g. 1901–2015 as used in this study is considered, the strength of the driving forces may be lower than expected due to the cancellation of the negative and positive influences over different data periods (Onyutha 2016b).

4 Conclusions

Studies dealing with analyses of trends in precipitation over Africa tend to be confined to sub-regions and are mainly based on short-term data. This paper assessed trends in precipitation over the entire continent of Africa using data of high spatial resolution ($0.5° \times 0.5°$) and long-term period (1901–2015). The trend magnitude (mm/year) of precipitation over the period 1991–2015 was subtracted from that of the 1965–1990 to obtain Slope Difference (SD, mm/year). Co-variation of the precipitation sub-trends with changes in large-scale ocean-atmospheric conditions was investigated.

Over the full period 1901–2015, precipitation at most grid points exhibited an increase in the March–May (MAM) and June–August (JJA) seasons. However, in most parts of Africa, there was a decrease in the annual, December–February (DJF), and September–November (SON) precipitation. The null hypothesis H_0 (no trend) was rejected ($p < 0.05$) for a positive trend in annual precipitation at more locations over the period 1991–2015 than those of 1965–1990. This means the continent was, on average, recently (from 1965 to 1990) wetter than it was

over the period 1965–1990. In both annual and seasonal precipitation, the lowest SD values (in the range -1 to 1 mm/year) were in areas north of 10° N. For the MAM precipitation, negative SD values (of about -5 mm/year) were obtained in the Horn of Africa. For the peak monsoon (JJA), the SD over the Sahel belt went up to about 20 mm/year. For the JJA precipitation, large SD values were confined to areas south of the Equator.

In East Africa, variability in SON precipitation was positively correlated with IOD and AMO. Over West Africa, JJA, SON and annual precipitation was correlated with AMO. Niño 3 was positively (negatively) correlated with South African SON (DJF) precipitation. MAM precipitation in the southern Africa was positively correlated with IOD. These findings show that the rainfall distribution across each region of Africa may be influenced by the changes in SST or SLP from various oceans. Of course, the amount of contribution of the driving influence varies in magnitude from one ocean to another, and perhaps even across the various regions of an ocean.

It is vital to acknowledge a number of limitations of this study. The accuracy in the process of interpolation through which the CRU data used in this study was obtained depends on the density of the weather stations and data availability in both space and time. This means that the accuracy of the trend results might have varied across the continent. The relationship between precipitation variability and possible predictor (a climate index) was assumed to be in a linear way. It is possible that such a relationship can be non-linear. Therefore, the use of other models (apart from linear regression) in predicting the variation of sub-trends in precipitation could be explored. Such statistical forecasts could be done while taking into perspective the seasonal predictability of precipitation (across the various regions of Africa) with the possible lead times of the circulation variables. Changes in precipitation may lag or precede the changes in SST or SLP by a number of months or even years. The lag or precedence of changes in the large-scale ocean-atmospheric conditions by the precipitation variability was not considered in this study, yet it can potentially influence the spatial results of the correlation between precipitation and climate indices. The results of co-variation of precipitation variability and climate indices were based only 15-year sub-trends. Perhaps, the use of another relevant time scale such as 10, 30-year, etc. would influence the spatio-temporal results of the correlation analyses. Furthermore, the correlation between precipitation sub-trends and climate indices may merely indicate statistical measure of association. It may not, for various factors (for instance, the high signal-to-noise ratio, inter-correlation among the climate indices) be so indicative of the actual dynamics of how the SST or SLP from various oceanic regions shape precipitation distribution across Africa. It would be vital to do an in-depth assessment of the influence of climate drivers on African precipitation using various short data periods chosen from a long-term series. In doing so, which mechanisms drove precipitation of various African regions over certain periods would be explored (something which, for brevity, was not done in this study). With respect to the regional precipitation distribution and variability across Africa, further exploration should be made on: the effect of possible interactions between regional circulation (e.g. localized convergence) with local geographical factors (including high lands, lakes, etc.), the interaction (if any) between remote forcing (such as Walker circulation, El Niño Southern Oscillation, and Indian Ocean Dipole) with the coastal influences (like coastal SST, and frictional uplift), the influence of possible regional-based feedback between land surface and atmosphere, etc.

Despite the above limitations (which may be addressed in future research using climate datasets that can accurately reproduce observed precipitation trends and variability across the entire African continent), the findings from this study are vital for an insight on: (1) the significance of both trend directions and magnitudes, (2) acceleration/deceleration of the precipitation increase/decrease, and (3) the co-variation of precipitation sub-trends and possible predictors to support careful planning of predictive adaptation.

Acknowledgements The data series used in this study were obtained from the Climatic Research Unit (CRU) (i.e. Time-Series (TS) Version 4.0 or CRU TS4.0). The author wishes to thank the four reviewers for their thorough comments and suggestions. The codes or tools (such as CSD-NAIM and CSD-VAT) used in this study were downloaded online via the link: https://sites.google.com/site/conyutha/tools-to-download (accessed: 18 July 2018).

Compliance with ethical standards

Conflict of interest The author declares no conflict of interest and no competing financial interests.

Appendix A

See Fig. 8.

Fig. 8 African countries. (Source: Nations Online Project [NOP] 2017)

References

Adler RF, Huffman GF, Chang A, Ferraro R, Xie P-P, Janowiak J, Rudolf B, Schneider U, Curtis S, Bolvin D, Gruber A, Susskind J, Arkin P, Nelkin E (2003) The version-2 global precipitation climatology project (GPCP) monthly precipitation analysis (1979-present). J Hydrometeorol 4:1147–1167

Anderson RL (1941) Distribution of the serial correlation coefficients. Ann Math Stat 8:1–13

ArcGIS (2017) Africa map of Köppen climate classification. http://www.arcgis.com/. Accessed 21 Aug 2017

Balas N, Nicholson SE, Klotter D (2007) The relationship of rainfall variability in West Central Africa to sea surface temperature fluctuations. Int J Clim 27:1335–1349

Bergonzini L, Richard Y, Petit L, Camberlin P (2004) Zonal circulations over the Indian and Pacific oceans and the level of Lakes Victoria and Tanganyika. Int J Climatol 24(13):1613–1624

Brandt M, Mbow C, Diouf AA, Verger A, Samimi C, Fensholt R (2014) Ground and satellite based evidence of the biophysical mechanisms behind the greening Sahel. Global Change Biol 21:1–11

Bunting AH, Dennett MD, Elston J, Milford JR (1976) Rainfall trends in the West African Sahel. Q J R Meteorol Soc 102:59–64

Camberlin P (2009) Nile basin climates. In: Dumont HJ (ed) The Nile: origin, environments, limnology and human use, monographiae biologicae, vol 89. Springer, Dordrecht, pp 307–333

Climate Data Guide (2017) CRU TS Gridded precipitation and other meteorological variables since 1901. https://climatedataguide.ucar.edu/climate-data/cru-ts-gridded-precipitation-and-other-meteorological-variables-1901. Last accessed 16 Aug 2017

Diem JE, Ryan SJ, Hartter J, Palace MW (2014) Satellite-based rainfall data reveal a recent drying trend in central equatorial Africa. Clim Change 126(1–2):263–272

Dong B, Sutton R (2015) Dominant role of greenhouse-gas forcing in the recovery of Sahel precipitation. Nat Clim Change 5:757–760

Dong B, Sutton RT, Highwood E, Wilcox L (2014) The impacts of European and Asian anthropogenic sulfur dioxide emissions on Sahel precipitation. J Clim 27:7000–7017

Fauchereau N, Trzaska S, Rouault M, Richard Y (2003) Rainfall variability and changes in Southern Africa during the 20th century in the global warming context. Nat Hazards 29(2):139–154

Giannini A, Biasutti M, Held IM, Sobel AH (2008) A global perspective on African climate. Clim Change 90(4):359–383

Goddard L, Graham NE (1999) Importance of the Indian Ocean for simulating rainfall anomalies over eastern and southern Africa. J Geophys Res 104(D16):19099. https://doi.org/10.1029/1999JD900326

Grimes DIF, Coppola E, Verdecchia M, Visconti G (2003) A neural network approach to real-time rainfall estimation for Africa using satellite data. J Hydrometeorol 4(6):1119–1133

Harris I, Jones PD, Osborn TJ, Lister DH (2014) Updated high-resolution grids of monthly climatic observations–the CRU TS3.10 dataset. Int J Climatol 34:623–642

Huffman GJ, Bolvin DT, Nelkin EJ, Wolff DB (2007) The TRMM multisatellite precipitation analysis (TMPA): quasi-global, multiyear, combined-sensor precipitation estimates at fine scales. J Hydrometeorol 8:38–55

IPCC (2007) Climate change 2007: the physical science basis, working group 1, IPCC fourth assessment report, Cambridge University Press, Cambridge and New York, pp 996

IWMI (2014) East Africa. http://eastafrica.iwmi.cgiar.org/. Retrieved 01 Feb 2014)

Janowiak JE (1988) An investigation of interannual rainfall variability in Africa. J Clim 1(3):240–255

Jones PD, Jonsson T, Wheeler D (1997) Extension to the North Atlantic oscillation using early instrumental pressure observations from Gibraltar and south-west Iceland. Int J Climatol 17(13):1433–1450

Jury MR (2013) Climate trends in southern Africa. S Afr J Sci 109(1/2):1–11

Kaptué AT, Hanan NP, Prihodko L, Ramirez JA (2015) Spatial and temporal characteristics of precipitation in Africa: summary statistics for temporal downscaling. Water Resour Res 51:2668–2679

Kendall MG (1975) Rank correlation methods, 4th edn. Charles Griffin, London

Korecha D, Barnston AG (2007) Predictability of June–September precipitation in Ethiopia. Mon Weather Rev 135:628–650

Kruger AC, Nxumalo MP (2017) Historical rainfall trends in South Africa: 1921–2015. Water SA. https://doi.org/10.4314/wsa.v43i2.12

Kundzewicz ZW, Robson AJ (2004) Change detection in hydrological records—a review of the methodology. Hydrol Sci J 49:7–19

Landman WA, Beraki A (2012) Multi-model forecast skill for mid-summer rainfall over southern Africa. Int J Climatol 32(2):303–314

Lebel T, Ali A (2009) Recent trends in the Central and Western Sahel rainfall regime (1990–2007). J Hydrol 375(1–2):52–64

Liebmann B, Hoerling MP, Funk C, Bladé I, Dole RM, Allured D, Quan X, Pegion P, Eischeid JK (2014) Understanding recent eastern Horn of Africa rainfall variability and change. J Clim 27(23):8630–8645

Lindesay JA (1988) South African rainfall, the southern oscillation and a southern hemisphere semi-annual cycle. J Climatol 8(1):17–30

Lyon B, DeWitt DA (2012) A recent and abrupt decline in the East Africa long rains. Geophys Res Lett 39:L02702. https://doi.org/10.1029/2011GL050337

Maidment RI, Grimes D, Allan RP, Tarnavsky E, Stringer M, Hewison T, Roebeling R, Black E (2014) The 30 year TAMSAT African rainfall climatology and time series (TARCAT) data set. J Geophys Res Atmos 119:10619–10644

Maidment RI, Allan RP, Black E (2015) Recent observed and simulated changes in precipitation over Africa. Geophys Res Lett 42:8155–8164

Mann HB (1945) Nonparametric tests against trend. Econometrica 13(3):245–259

Meyer-Christoffer A, Becker A, Finger P, Rudolf B, Schneider U, Ziese M (2011) GPCC climatology version 2011 at 0.25°: monthly land-surface precipitation climatology for every month and the total year from rain-gauges built on GTS-based and historic data. https://doi.org/10.5676/dwd_gpcc/clim_m_v2011_025

Nicholson SE (1996) A review of climate dynamics and climate variability in Eastern Africa. In: Johnson TC, Odada EO (eds) The limnology, climatology and paleoclimatology of the East African Lakes. Gordon and Breach, Amsterdam, pp 25–56

Nicholson SE (2000) The nature of rainfall variability over Africa on time scales of decades to millenia. Glob Planet Change 26:137–158

Nicholson SE (2001) Climatic and environmental change in Africa during the last two centuries. Clim Res 17(2):123–144

Nicholson SE (2015) Long-term variability of the East African "short rains" and its links to large-scale factors. Int J Climatol 35(13):3979–3990

Nicholson SE (2017) Climate and climatic variability of rainfall over Eastern Africa. Rev Geophys 55(3):590–635

Nicholson SE, Selato JC (2000) The influence of La Nina on African rainfall. Int J Climatol 20:1761–1776

NOP (2017) Map of the African continent with countries, main cities and capitals. http://www.nationsonline.org/oneworld/map/africa-political-map.htm. Retrieved 02 Jun 2017

Novella NS, Thiaw WM (2013) African rainfall climatology version 2 for famine early warning systems. J Appl Meteorol Climatol 52(3):588–606

Ogallo L (1979) Rainfall variability in Africa. Mon Weather Rev 107(9):1133–1139

Ogwang BA, Chen H, Tan G, Ongoma V, Ntwali D (2015) Diagnosis of East African climate and the circulation mechanisms associated with extreme wet and dry events: a study based on RegCM4. Arab J Geosci 8:10255–10265

Omondi PA, Awange JL, Forootan E, Ogallo LA, Barakiza R, Girmaw GB, Fesseha I, Kululetera V, Kilembe C, Mbati MM, Kilavi M, King'uyu SM, Omeny PA, Njogu A, Badr EM, Musa TA, Muchiri P, Bamanya D, Komutunga E (2014) Changes in temperature and precipitation extremes over the Greater Horn of Africa region from 1961 to 2010. Int J Climatol 34(4):1262–1277

Onyutha C (2016a) Statistical analyses of potential evapotranspiration changes over the period 1930–2012 in the Nile River riparian countries. Agric For Meteorol 226–227:80–95

Onyutha C (2016b) Identification of sub-trends from hydro-meteorological series. Stoch Env Res Risk Assess 30:189–205

Onyutha C (2016c) Statistical uncertainty in hydro-meteorological trend analyses. Adv Meteorol 2016:1–26. https://doi.org/10.1155/2016/8701617

Onyutha C (2017) On rigorous drought assessment using daily time scale: Non-stationary frequency analyses, revisited concepts, and a new Method to yield non-parametric indices. Hydrology 4:48. https://doi.org/10.3390/hydrology4040048

Onyutha C, Willems P (2015) Spatial and temporal variability of rainfall in the Nile Basin. Hydrol Earth Syst Sci 19(5):2227–2246

Onyutha C, Willems P (2017a) Influence of spatial and temporal scales on statistical analyses of rainfall variability in the River Nile basin. Dyn Atmos Oceans 77(C):26–42

Onyutha C, Willems P (2017b) Space-time variability of extreme rainfall in the River Nile basin. Int J Climatol 37(4):4915–4924

Onyutha C, Tabari H, Taye MT, Nyandwaro GN, Willems P (2016) Analyses of rainfall trends in the Nile River Basin. J Hydro-Env Res 13:36–51

Rayner NA, Parker DE, Horton EB, Folland CK, Alexander LV, Rowell DP, Kent EC, Kaplan A (2003) Global analyses of sea surface temperature, sea ice, and night marine air temperature since the late nineteenth century. J Geophys Res 108(D14):4407

Reason CJC, Allan RJ, Lindesay JA, Ansell TJ (2000) ENSO and climatic signals across the Indian Ocean Basin in the global context. Part I: Interannual composite patterns. Int J Climatol 20(11):1285–1327

Robson A, Bardossy A, Jones D, Kundzewicz ZW (2000) Statistical methods for testing for change. In: Kundzewicz ZW, Robson A (eds) Detecting trend and other changes in hydrological data. World Meteorological Organization, Geneva, pp 46–62

Rowell DP, Folland CK, Maskel K, Ward MN (1995) Variability of summer rainfall over tropical north Africa 1906–92: observations and modelling. Q J R Meteorol Soc 121:669–704

Rowell DP, Booth BB, Nicholson SE, Good P (2015) Reconciling past and future precipitation trends over the East Africa. J Clim 28:9768–9788

Salas JD, Delleur JW, Yevjevich V, Lane WL (1980) Applied modelling of hydrologic time series. Water Resources Publications, Littleton, p 484

Sen PK (1968) Estimates of the regression coefficient based on Kendall's tau. J Am Stat Assoc 63:1379–1389

Sheffield J, Goteti G, Wood EF (2006) Development of a 50-year high-resolution global dataset of meteorological forcings for land surface modeling. J Clim 19(13):3088–3111

Ta S, Kouadio KY, Ali KE, Toualy E, Aman A, Yoroba F (2016) West Africa extreme rainfall events and large-scale ocean surface and atmospheric conditions in the tropical atlantic. Adv Meteorol. https://doi.org/10.1155/2016/1940456

Tarnavsky E, Grimes D, Maidment R, Black E, Allan RP, Stringer M, Chadwick R, Kayitakire F (2014) Extension of the TAMSAT satellite based rainfall monitoring over Africa and from 1983 to present. J Appl Meteorol Climatol 53(12):2805–2822

Theil H (1950) A rank-invariant method of linear and polynomial regression analysis. Nederl Akad Wetench Ser A 53:386–392

Tierney JE, Smerdon JE, Anchukaitis KJ, Seager R (2013) Multidecadal variability in East African hydroclimate controlled by the Indian Ocean. Nature 493:389–392

Tierney JE, Ummenhofer CC, deMenocal PB (2015) Past and future precipitation in the Horn of Africa. Sci Adv 1(9):e1500682. https://doi.org/10.1126/sciadv.1500682

Trenberth KE (1997) The definition of El Nino? Bull Am Meteorol Soc 78(12):2771–2777

van Oldenborgh GJ, te Raa LA, Dijkstra HA, Philip SY (2009) Frequency- or amplitude-dependent effects of the Atlantic meridional overturning on the tropical Pacific Ocean. Ocean Sci 5:293–301

Villamayor J, Mohino E (2015) Robust sahel drought due to the interdecadal Pacific oscillation in CMIP5 simulations. Geophys Res Lett 42:1214–1222

Washington R, Preston A (2006) Extreme wet years over southern Africa: role of Indian Ocean sea surface temperatures. J Geophys Res 111:D15104. https://doi.org/10.1029/2005JD006724

Washington R, James R, Pearce H, Pokam WM, Moufouma-Okia W (2013) Congo basin rainfall climatology: Can we believe the climate models? Philos Trans R Soc Lond Ser B. https://doi.org/10.1098/rstb.2012.0296

Williams A, Funk C (2011) A westward extension of the warm pool leads to a westward extension of the Walker circulation, drying Eastern Africa. Clim Dyn 37:2417–2435

WMO (2000) Detecting trend and other changes in hydrological data. In: Kundzewicz ZW, Robson A (Eds.) World climate programwater. WMO/UNESCO, WCDMP-45, WMO/TD-No.1013, Geneva

Zhang R, Delworth TL (2006) Impact of Atlantic multidecadal oscillations on India/Sahel rainfall and Atlantic hurricanes. Geophys Res Lett. https://doi.org/10.1029/2006GL026267